Water-Induced Micelle Formation of Block Copoly(oxyethylene–oxypropylene–oxyethylene) in *o*-Xylene

Guangwei Wu, Zukang Zhou, and Benjamin Chu*

Chemistry Department, State University of New York at Stony Brook, Long Island, New York 11794-3400

Received June 18, 1992; Revised Manuscript Received January 11, 1993

ABSTRACT: Static and dynamic light scattering, viscometry, NMR, and vapor pressure osmometry techniques have been employed to study the water-induced micellization behavior of poly(oxyethylene–oxypropylene–oxyethylene) block copolymer, Pluronic L64, in *o*-xylene solution. Results show that Pluronic L64 does not form polymolecular micelles in the absence of water or in the presence of a small amount of water (molar ratio water/EO < 0.15). Micelles, consisting of a PPO shell and a PEO and H_2O core, are formed when the water to EO molar ratio (Z) in the micelle is greater than 0.2. For $Z < 1.3$, spherical micelles with an average hydrodynamic radius R_h of ca. 9.2 nm are formed, with R_h almost independent of Z. For $Z > 1.3$, both the aggregation number and the hydrodynamic radius become dependent on the Z value, then the micelle shape could be nonspherical. As experimentally evidenced by NMR spectra, the solubilized water can be classified into bound water and free water. Most likely, water is not evenly distributed in the core, as the environments of EO units at different positions in the block copolymer are not identical.

Introduction

Poly(oxyethylene–oxypropylene–oxyethylene) (PEO–PPO–PEO) triblock copolymers (trade name Pluronic) are widely used nonionic surfactants.[1] Micellar properties can be changed to meet specific requirements in different areas by varying the block length and the weight ratio of PEO to PPO. They have attracted considerable attention in both fundamental research and practical application. In general, the colloidal behavior of block copolymers of ABA type in solution is still not very clear due to the complexity of their conformation, interaction, and composition. There have been a number of studies dealing with PEO–PPO–PEO ABA block copolymers in water,[2-12] which is a good solvent for the end blocks (PEO). It is now well-known that EPE type block copolymers can form micelles in water at a proper concentration region and temperature range. The micelle consists of a PEO shell and a PPO core. The micelle size and shape are closely related to the temperature, pressure, concentration, solubilizates, and the composition of the block copolymer. Temperature plays a very important role with respect to the micellization and the micelle size. For some systems,[2] there exist three temperature regions, i.e. unimer region, transition region, and micelle region. Temperature variation affects the solvation of PEO and thereby the aggregation number of the micelle. At high concentrations, gelation is possible for some copolymers, e.g. Pluronic F127 and P85.[5a,6] The behaviors of Pluronic copolymers in water at high concentrations were well described by using a hard sphere model.[6] The organic solubilizate was found to play an important role with respect to the micelle size.[3] The micelle size and the aggregation number increase as the amount of solubilization is increased.

To our knowledge, few studies were reported on the micellization behavior of Pluronic block copolymers in nonaqueous solvents. Cowie and Sirianni[13] studied Pluronic F38, F68, F88, and F108 in benzene and dioxane by light scattering, vapor pressure osmometry, and ultracentrifugation. They found that polyols can form micelles in benzene and dioxane at 37 °C. The aggregation number of F68 in benzene was about 4. The effect of a trace amount of water was marked. The aggregation number of F68 in water-saturated benzene was nearly double that in dry benzene. They suggested that the micelle was nonspherical. Very recently, Samii et al.[14] studied the phase behavior of PEO–PPO block copolymers in nonaqueous solvents. Hydrogen bonding between solvent and copolymer plays a very important role with respect to the solution properties of the block copolymers.

Although the behavior of PEO–PPO–PEO block copolymers in apolar solvents is rarely studied, the behavior of nonionic surfactants of the type of poly(ethylene glycol) alkyl ether has been well investigated.[15-18] Ravey et al.[16] classified nonaqueous solvents into three classes and reported that only unimers or possibly a few dimers exist in aromatic solvents. Water plays an important role in the micellization and the micelle structure of nonionic surfactants in organic solvents. For example, the aggregation number of $C_{12}(EO)_4$ in decane is about 10 at 20 °C but increases to 500–700 after water solubilization. With an increase in solubilized water, the structure of the micelle changes from hank-like (interpenetrated bilayers) to lamellar (separated bilayers). After the EO group was fully hydrated (H_2O/EO = 2–3), further addition of water would create a central aqueous film. Cooney et al.[17] used Raman spectroscopy to study the Triton X-100/benzene/water system. They found that water could form 1:1 hydrogen bonds with the EO group in Triton X-100. This formation has priority over the formation of water–water hydrogen bonds. Christenson et al.[18] studied the interaction between water and EO of poly(ethylene glycol) dodecyl ether in the hydrocarbon media by NMR and light scattering. They concluded that there was no association at low water concentration. At a water/EO ratio between 0.6 and 1.4, association structures started to form. The average chain conformation changed with the water content. At higher water concentrations, a water-rich core was formed. The chemical shift of the water proton increases quickly first and then tends toward a constant with a further increase in the amount of water.

Both PEO–PPO–PEO copolymers and poly(ethylene glycol) alkyl ethers have the same lyophobic part (PEO) in apolar solvents. In principle, it is possible that they would have similar colloidal properties. However, in literature there is certainly a lack of information on the behavior of Pluronic block copolymers in nonaqueous media. Whether they can form micelles in apolar solvents

* Author to whom correspondence should be addressed.

0024-9297/93/2226-2117$04.00/0

and how the water can affect the micellization behavior are the important basic questions. We have systematically investigated the association properties of Pluronic L64 in water[2] and the effect of solubilized *o*-xylene on the micelle structure.[3] In this work, we present some results on Pluronic L64 in *o*-xylene (a good solvent for the middle PPO block) with and without the presence of water, using static and dynamic light scattering, NMR, VPO, and viscometry. L64 is a typical Pluronic surfactant consisting of 60% by weight of PPO, and the length of the hydrophobic block is nearly the same as the total length of the hydrophilic part. We want to further expand our study of the colloidal properties of this typical block copolymer to organic media, with our attention being concentrated on the effect of solubilized water. It would be very interesting if the size and the structure of micelle can be controlled by varying the amount of solubilized water.

Recently, Rodrigues and Mattice[23] reported a computer simulation of the behavior of a triblock copolymer $B_5A_{10}B_5$ in a solvent which is a good solvent for the middle block. Their results show that the micelle has a rudimentary internal core consisting of dense-packed beads of B, a very diffuse interface, and an expanded corona. Cogan and Gast[24] have studied the effect of water on PS–PEO diblock copolymers in cyclopentane, a select solvent for polystyrene. A trace amount of water can markedly increase the aggregation number of the micelle. Further addition of water results in a solution of swollen micelles, i.e. a polymeric microemulsion.

Experimental Methods

Materials and Solution Preparation. Pluronic L64 was obtained from BASF and used without further purification. The nominal molar mass of this copolymer is 2900 g mol^{-1}. HPLC grade *o*-xylene and *o*-xylene-d_{10} (99+ atom % D) were purchased from Aldrich Co. and used as received. The solution was prepared by first making a concentrated solution. After standing overnight, the solution was diluted to the required concentration. The solution for light scattering measurements was clarified by filtration through a 0.2-μm pore size Millipore filter. To solubilize water, clarified distilled water was added to the filtered L64/*o*-xylene solution. The solutions for NMR measurements were made by first dissolving L64 in *o*-xylene-d_{10} and then adding the proper amounts of water.

Solubilization Measurements. We used two ways to measure the maximum solubilized amount of water in L64/*o*-xylene solution. The first one was to use a microsyringe (5 or 10 μL) to add an increasing amount of water to the solution until the solution became cloudy and remained so within 10 min for most of the L64 concentrations. The second way was to make a water-solubilized L64/*o*-xylene solution by adding a known amount of water to the solution, and then by diluting the solution with further addition of solvent *o*-xylene till the solution became cloudy. In the vicinity of the critical micelle concentration (cmc), the equilibration time required was much longer. The solubilization experiment was carried out at room temperatures (23–24 °C).

Refractive Index Increment. The refractive index increment $(dn/dC)_{T,P}$ was determined by using a Brice-Phoenix differential refractometer. Measurements were made at 26.2 °C and at wavelengths of 436 and 546 nm. From the measured values, the refractive index increments at 488 nm were obtained by interpolation. Thus $dn/dC = -0.045$ cm^3 g^{-1} for the L64/*o*-xylene system. For the L64/water/*o*-xylene system, $dn/dC = -0.050 - 0.012Z$ cm^3 g^{-1}, where Z is the molar ratio of water to ethylene oxide (EO) units in the micelle.

Static Light Scattering. A standard, laboratory-built spectrometer[19] was used to measure the scattered light intensity and to perform photon correlation measurements at scattering angles between 20 and 135°. A Spectra-Physics argon ion laser (Model 165) was operated at 488 nm with an output power in the 200–400-mW range. The cell was held in a brass thermostat whose temperature was controlled to ±0.02 °C. We used benzene as a reference for computing the Rayleigh ratio R_{vv} of the sample solution with $R_{vv}(T) = 32.0 \times 10^{-6}[1 + 3.68 \times 10^{-3}(T - 298)]$ cm^{-1} for benzene at 488 nm.[19]

The excess Rayleigh ratio (R_{vv}) for vertically polarized incident and scattered light has the form

$$R_{vv} = HCM^*P(q)S(q,C) \tag{1}$$

$H = 4\pi^2n^2(dn/dC)^2_{T,P}/(N_A\lambda_0^4)$, where n is the refractive index of the solution, N_A, Avogadro's number, λ_0, the wavelength of the incident light in vacuo, and C, the concentration of the solute in g cm^{-3}. $P(q)$ and $S(q,C)$ are the form factor and the structure factor, respectively, with q $[=(4\pi n/\lambda_0)\sin(\theta/2)]$ being the magnitude of the scattering vector. The apparent molar mass (M^*) is equal to the weight average molar mass (M_w) if the refractive indices of the two blocks are equal.[20] For a system heterogeneous in composition, the apparent molar mass and the weight average molar mass are related by

$$M^*(dn/dC)^2 = M_w(dn/dC)_A(dn/dC)_B + [(dn/dC)_A^2 - (dn/dC)_A(dn/dC)_B]W_AM_{w/A} + [(dn/dC)_B^2 - (dn/dC)_A(dn/dC)_B]W_BM_{w/B} \tag{2}$$

with $M_{w/A}$ and $M_{w/B}$ being the weight-average molecular weights of the components A and B and W_A and W_B being the weight-average weight fractions of A and B, respectively. For L64, the refractive indices of the two components (PEO and PPO) are very close, 1.4563 and 1.4495, respectively, at the sodium D line. They also have similar densities. Thus the difference between the apparent molar mass and the weight-average molar mass is estimated to be only ca. 1%. For our system, the particle size was small, i.e. $qR_g \ll 1$. Therefore, we did not observe the angle dependence of scattered intensity and can simply let $P(q) = 1.0$. The structure factor $S(q,C)$ reflects the particle–particle interaction. One of the simplest models for repulsive interaction is the so-called hard sphere (HS) model. Based on the Percus–Yevick approximation,[27] the structure factor at a finite concentration and zero scattering angle can be expressed as

$$S(q=0,C) = (1 - \varphi)^4(1 + 2\varphi)^{-2} \tag{3}$$

where φ is the volume fraction of the hard spheres and is related to the solute concentration by $\varphi = (4\pi R_{HS}^3/3M)N_AC$, with R_{HS} the radius of hard sphere. In the dilute solution region, eq 1 can be approximated as

$$HC/R_{vv} = 1/M^* + 2A_2C + \ldots \tag{4}$$

where A_2 is the second virial coefficient. For a micellar solution, eq 4 should be written as

$$H(C - \mathrm{cmc})/R_{vv} = 1/M^* + 2A_2(C - \mathrm{cmc}) \tag{4B}$$

where M^* is the apparent molar mass of the micelle and cmc is the critical micelle concentration.

In the intermediate concentration region, a combination of eqs 1 and 3 leads to (in the logarithmic form)

$$\log(HC/R_{vv}) = -\log(M^*) + 3.48\varphi \tag{4C}$$

The error caused by neglecting the higher-order terms of $\log(S(q=0,C))$ is less than 5% up to $\varphi \sim 0.4$.

Photon Correlation Speectroscopy. The intensity autocorrelation function was measured at various scattering angles in the range 20–135° with a Brookhaven BI2030AT 64-channel digital correlator. When the measured and the calculated baselines were in good agreement (difference <0.1%), the correlation function was accepted. The measured correlation function in the self-beating mode has the form

$$G^{(2)}(q,\tau) = A(1 + \beta|g^{(1)}(q,\tau)|^2) \tag{5}$$

with τ, the delay time, A, the background, and β, the coherence factor. The measured electric field correlation function $|g^{(1)}(q,\tau)|$

was fitted with a cumulants expansion

$$g^{(1)}(q,\tau) = \exp\{-\bar{\Gamma}(q)\tau + 0.5\mu_2(q)\tau^2 + ...\} \quad (6)$$

where $\bar{\Gamma}$ is the mean line width and $\mu_2/\bar{\Gamma}^2$ is the variance of the line width distribution function. From $\bar{\Gamma}$, the z-average translational diffusion coefficient (D) is obtained:

$$D = \bar{\Gamma}/q^2 \quad (7)$$

By extrapolation of the values for the diffusion coefficient to zero concentration (D_0), the average hydrodynamic radius (R_h) can be calculated by using the Stokes–Einstein relation,

$$R_h = k_B T/(6\pi\eta D_0) \quad (8)$$

where k_B, T, and η are the Boltzmann constant, the absolute temperature, and the solvent viscosity, respectively.

Viscosity. The viscosity of the copolymer solution was determined by using either an Ubbelohde type multibulb capillary viscometer or a Brookfield cone–plate viscometer with a shear rate ranging from 1.15 to 230.0 s^{-1}. From the measured viscosity, we can calculate the intrinsic viscosity $[\eta]$ of the system by using either

$$(\eta_r - 1)/C = [\eta] + k_1[\eta]^2 C + ... \quad (9)$$

or

$$\ln(\eta_r)/C = [\eta] + k_2[\eta]^2 C + ... \quad (10)$$

where η_r ($= \eta_{solu}/\eta_{solv}$) is the relative viscosity, C is the concentration of solute in g cm^{-3}, and k_1 and k_2 are Huggins' and Kramer's coefficients, respectively. For a dilute polymer solution, $k_1 - k_2 = 0.5$. k_1 or k_2 reflects the interaction of the particle with the solvent. The intrinsic viscosity $[\eta]$ is related to the particle shape and density by the expression[21]

$$[\eta] = \nu/\rho^* = \nu(\rho_p^{-1} + \zeta\rho_s^{-1}) \quad (11)$$

where ν is the shape factor, ζ is the degree of solvation (solvated solvent weight per gram of polymer), and ρ^*, ρ_p, and ρ_s are the density of the particle, polymer, and solvent respectively. For spheres, $\nu = 2.5$; for ellipsoids, $\nu > 2.5$.

Knowing $[\eta]$ and assuming that particles are spherical, one can calculate the radius of the equivalent hydrodynamic sphere (R_η) by[21]

$$R_\eta = \{3M[\eta]/(10\pi N_A)\}^{1/3} \quad (12)$$

NMR. A GE QE-300 NMR spectrometer was used to obtain the NMR results with tetramethylsilane as an internal reference. The chemical shift of the water proton observed (δ) is an average over different types of water protons because of the fast exchange of water protons

$$\delta = \sum \Phi_i \delta_i \quad (13)$$

where Φ_i and δ_i are the molar fraction and the chemical shift of component i, respectively.

Vapor Pressure Osmometry (VPO). A vapor pressure osmometer (Knauer) was used to determine the number average molecular weight (M_n) of L64 in o-xylene. The measured temperature difference and the solute concentration are related by

$$\Delta T = K(C/M_n + A_2C^2 + ...) \quad (14)$$

In the above formula, K and A_2 are the equipment constant and the second virial coefficient, respectively. We used sucrose octaacetate (FW = 678.60 g mol^{-1}) as a standard to calibrate the equipment constant.

Results and Discussion

Part A: L64/o-Xylene System. Light scattering, VPO, and viscometry were employed to investigate the behavior of L64 in anhydrous o-xylene. We used vapor pressure osmometry to determine the number-average molecular weight of L64 in o-xylene in the absence of water. The VPO results are shown in Figure 1. The number average

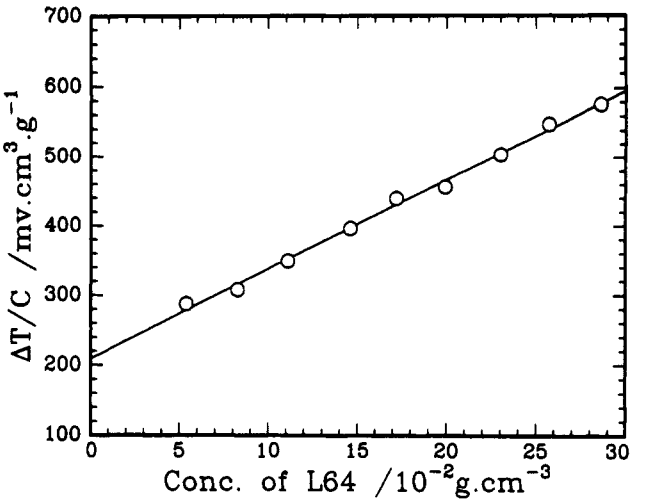

Figure 1. VPO results of L64 in o-xylene in the absence of water at 26.2 °C. The extrapolated intercept corresponds to an M_n of 3.4×10^3.

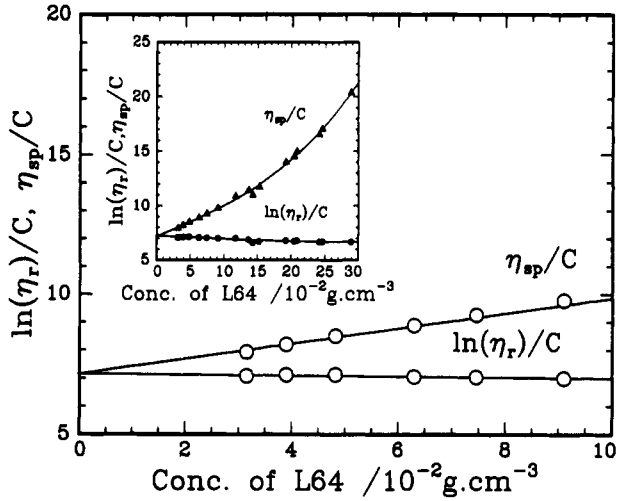

Figure 2. Viscosity results of L64 in o-xylene in the absence of water at 26.2 °C. Solid lines represent the fit by eqs 9 and 10. The derived intrinsic viscosity is 7.1 cm^3 g^{-1}. The inset covers a wider concentration range.

molecular weight (3.4×10^3 g mol^{-1}) obtained is close to the nominal value of 2900 g mol^{-1}, and $\Delta T/C$ versus C is linear in the concentration range of 0.05–0.28 g cm^{-3}, implying that in anhydrous o-xylene L64 exists as a unimer in this concentration range. Viscosity results are shown in Figure 2. There is no inflection within the entire concentration range studied, which is consistent with the VPO results. From the intrinsic viscosity value (7.10 cm^3 g^{-1}) and eq 11, we estimate that the possible maximum degree of solvation of L64 in o-xylene, ζ, would be 1.67 g/g, which corresponds to a molar ratio of xylene/PO of 1.5.

Our light scattering measurements further confirm that L64 exists essentially as unimers in anhydrous o-xylene. In the absence of angular dependence of scattered intensity, we can use the scattered intensity data measured at $\Theta = 90°$ directly. In Figure 3, HC/R_{90} is plotted against C. In the dilute region ($C < 0.10$ g cm^{-3}), HC/R_{90} versus C is linear. From the intercept and the slope of the plot, the molar mass of the L64 particle in o-xylene and the second virial coefficient were determined to be 3.7×10^3 g mol^{-1} and 4.5×10^{-3} mol cm^3 g^{-2}, respectively (see Table I). The weight-average molecular weight thus obtained is close to the above number-average molecular weight, yielding $M_w/M_n \approx 1.1$. A large value for the second virial coefficient strongly implies that the interaction between L64 chains is dominated by the repulsive forces,

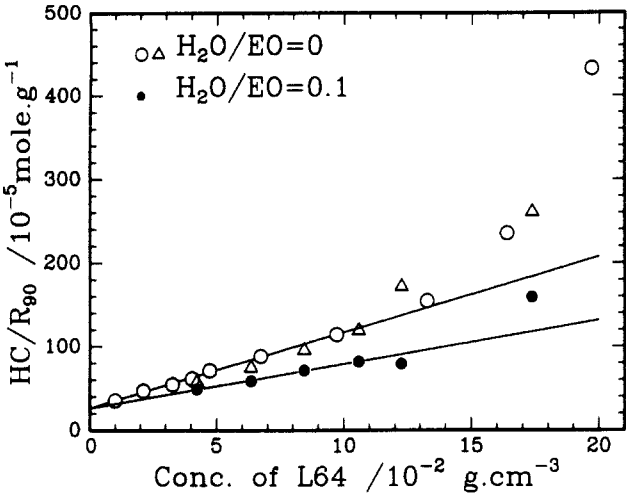

Figure 3. Concentration dependence of HC/R_{90} of L64 in *o*-xylene at 26.2 °C. The molar ratios of water to EO unit are 0 and 0.1, respectively.

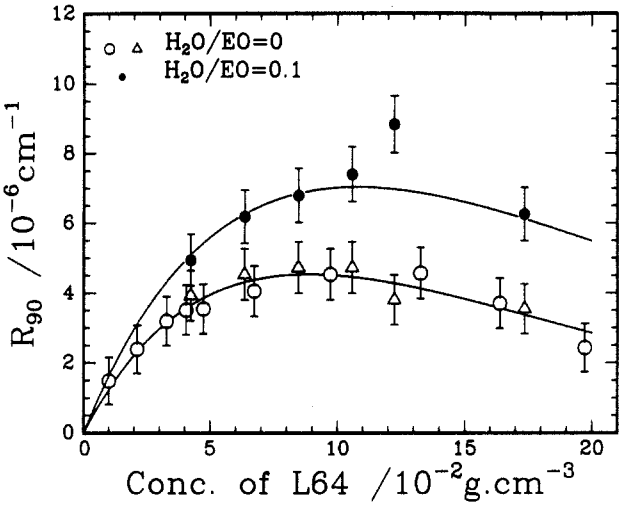

Figure 4. Excess Rayleigh ratio of L64 in *o*-xylene at 26.2 °C as a function of concentration of L64 in the absence of water (○, △) and in the presence of water (●). The solid lines are hard sphere fitting results based on eq 3.

Table I
Results of L64 in *o*-Xylene in the Absence of Water and in the Presence of a Small Amount of Water

H_2O/EO	M_w (g mol^{-1})	M_n (g mol^{-1})	R_{HS} (nm)	R_h (nm)	R_η (nm)	A_2 (mol cm^3 g^{-2})
0	3700	3400	1.2	1.4	1.6	0.0045
0.1	3800		1.3	1.7		0.0026

as does the above mentioned high degree of solvation of L64 in *o*-xylene. Although the HC/R_{90} versus C plot is no longer linear at higher concentrations because of the contribution of higher-order terms, there seems no inflection in the whole concentration range studied, as shown by the VPO and viscosity results. Thus, we expect that the unimer state has not changed in this concentration range. In order to probe the structure of the L64 unimer in *o*-xylene, we tried to use the hard sphere model to fit the experimental scattering data. In Figure 4, the relation of the excess Rayleigh ratio due to the L64 chains versus concentration is displayed. The lower solid line is the fitting result according to the hard sphere model (eq 3) with a hard sphere radius (R_{HS}) of 1.2 nm. The excess scattered intensity first increases and then decreases with increasing concentration. This behavior can be explained by the fact that the repulsive interactions between particles dominate. The hard sphere radius thus calculated agrees

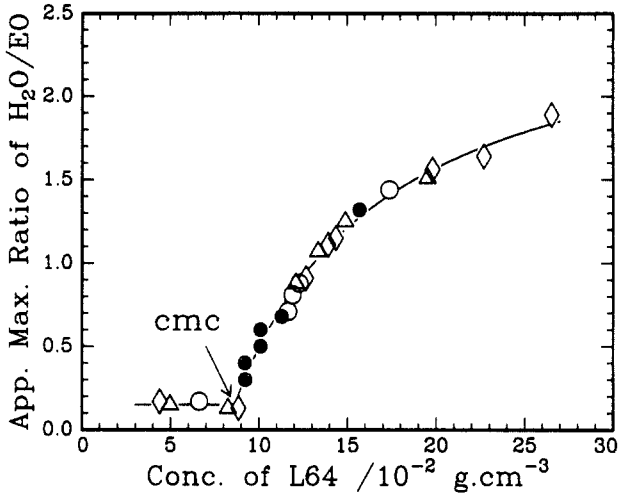

Figure 5. Apparent maximum ratio of solubilized water to EO against the concentration of L64 in *o*-xylene at room temperatures (23–24 °C). The solid line denotes the fitting results according to eq 15. Open symbols were measured by adding water to the solution till the solution becomes cloudy. The three open symbols represent three independent measurements. The filled symbol was measured by diluting the water-solubilized solution.

well with the measured hydrodynamic radius (R_h) of 1.4 nm, implying that, to a first order approximation, in the absence of water, L64 in *o*-xylene behaves like hard spheres.

From Figures 3 and 4 and Table I, we note that in the presence of a small amount of water with a molar ratio H_2O/EO of 0.1, the behavior of L64 in *o*-xylene is very similar to that in the anhydrous *o*-xylene. On the basis of the results of vicosity, VPO, and light scattering measurements, we can reach the conclusion that L64 does not form polymolecular micelles in the absence of water and even when a small amount of water is present. Most likely, the strong solvation of the PPO block by *o*-xylene prevents L64 from associating into micelles. The structure of L64 in *o*-xylene could be roughly approximated as a hard sphere. In *o*-xylene in the absence of water or in the presence of a small amount of water, the properties of L64 in *o*-xylene are very similar to those of the poly(oxyethylene) alkyl ether nonionic surfactants in aromatic solvents.[16,18] Our results differ from the report of Cowie and Sirianni.[13] The measured size of L64 unimer in *o*-xylene is comparable with previously reported values for L64 unimer in water: 1.7 nm by DLS[2] and 1.5 nm by NMR.[5]

Part B: L64/*o*-Xylene/Water System. (1) Solubilization of Water in L64/*o*-Xylene. Although L64 does not form micelles in anhydrous *o*-xylene, it can solubilize water remarkably well at higher concentrations (e.g. C >0.10 g cm^{-3}). The results of solubilization measurements are shown in Figure 5. In the low L64 concentration region, the amount of water solubilized, which is expressed as the molar ratio of solubilized water to oxyethylene (EO), is about 0.15, nearly independent of the L64 concentration. This solubilization is due to EO in each individual polymer hereafter referred to as the unimer. At higher concentrations, the apparent maximum amount of solubilized water per EO unit becomes much larger and is a function of the total L64 concentration, which is typical for micelle solubilization. Such behavior implies that, in the presence of water, L64 forms micelles at higher concentrations. To a first-order approximation, we may assume that the maximum ratio of solubilized water to EO units in L64 micelles is independent of the micelle concentration. Therefore, the experimentally measured apparent max-

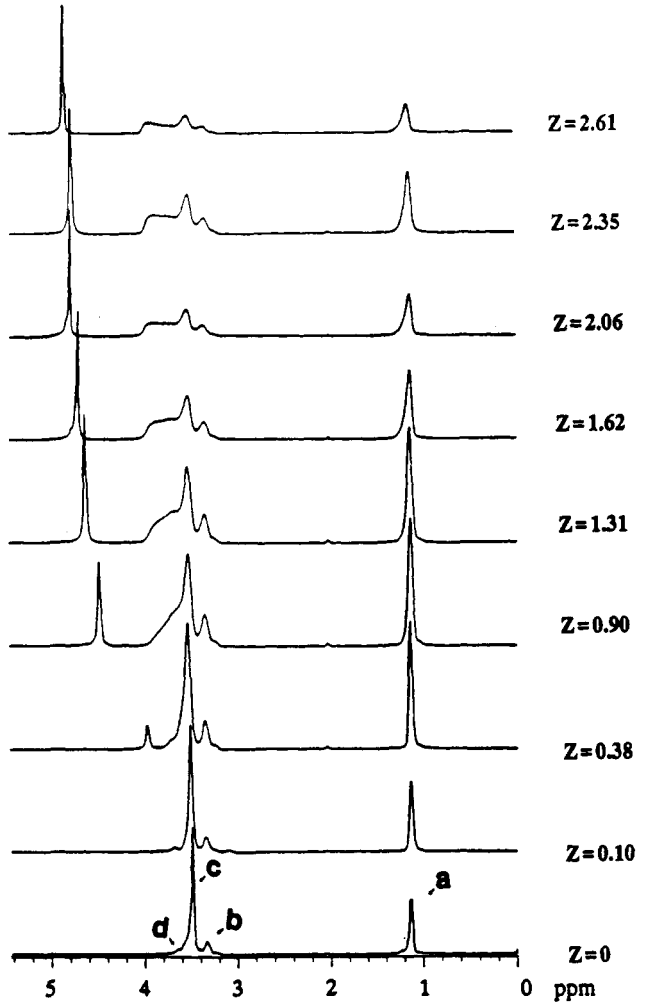

Figure 6. NMR spectra of L64 in *o*-xylene-d_{10} at different Z and at room temperature. The concentration of L64 is 0.316 g cm^{-3}.

imum molar ratio of solubilized water to EO (Z_{app}), as shown in Figure 5, can be approximately expressed by

$$Z_{app} = (Z_{max}(C - \text{cmc}) + Z_0\text{cmc})/C = Z_{max} - (Z_{max} - Z_0)\text{cmc}/C \quad (15)$$

where Z_{max} and Z_0 (=0.15) are the maximum molar ratio of solubilized water to EO in micelles and in the unimer, respectively. The solid curve in Figure 5 is the fit of eq 15. The fit agrees quite well with the experimental data in the high concentration region (C >0.11 g cm^{-3}), yielding cmc and Z_{max} values of 8.6 × 10^{-2} g cm^{-3} and 2.7, respectively. Data points obtained in two different ways, as described in the caption of Figure 5, agree quite well. It should be noted that, in the vicinity of the cmc, the time effect to reach equilibrium in solubilizing water was remarkable. It was difficult to get reproducible equilibrium results. In addition, the cmc for block copolymers usually represents a transition region. As a precautionary measure, all experimental data for further analysis were taken only in the high concentration region (C >0.11 g cm^{-3}).

(2) NMR Results. In order to understand the interaction between solubilized water and L64 molecules, we used NMR to study the environment change of water and EO of L64 from the proton spectra. Figure 6 shows the NMR spectra of L64 in *o*-xylene-d_{10} at different molar ratios of H_2O/EO in the micelle. In Figure 6, the peak a with chemical shift $\delta \approx 1.1$ ppm corresponds to the protons of the methyl group in oxypropylene; peak b with $\delta \approx 3.3$ ppm corresponds to the proton of the –CH< group in oxypropylene; peak b has one-third the area of peak a, thus having the same ratio as the chemical formula requires. This ratio further confirms that the assignment is reasonable. We assign peak c with $\delta \approx 3.5$ ppm to the resonance of the protons of methylene (–CH_2–) in both oxyethylene and oxypropylene. In the absence of water, the environments of the methylene protons (–CH_2–) of PO and EO are very similar. It is reasonable that they have the same chemical shifts. The peak d with $\delta \approx 3.62$ ppm shifts to lower field and becomes larger when more water is added. We assign this peak to the resonance of the hydroxyl proton of water. This assignment is reasonable when compared with the results of Christenson et al.[18]

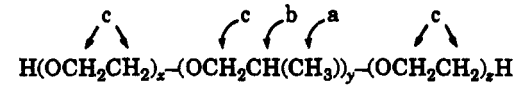

There is a resonance peak of the hydroxyl proton of water even without adding water to the system because both the L64 and solvent contain a trace amount of water. However, the corresponding characteristic peak is too small to permit a quantitative estimate of the amount of water. The chemical shifts of the methyl (peak a) and the –CH< (peak b) of the oxypropylene block remain essentially unchanged when the water to EO ratio in the micelle (Z) is increased from 0 to 1.3, implying that the chemical environment of the oxypropylene block has not changed. Thus, the penetration of water into the PPO shell is negligible in the region of $Z < 1.3$. When more water was solubilized, peak c exhibited a shoulder, which became broader with increasing Z. The methylene of EO could be responsible for this shoulder. If the environment of EO becomes more polar, the chemical shift should have a downfield shift.[18] With increasing Z, the chemical environments of EO units along the PEO chain are being changed. The degree of change is related to the location of the EO unit on the PEO chain and the amount of solubilized water. The EO unit in the most polar environment has the largest downfield shift. We can see, from the NMR spectra, that the environments (polarity) of EO units along the PEO chain are different after water solubilization, especially in the case of high Z, suggesting that water is not evenly distributed in the core of the micelle. Probably, the center of the core is richer in water than the interface region between PEO and PPO. Water is much more polar than the EO unit. The interface energy will increase if the water content in the interface is increased. Therefore the distribution with a water-rich core is an energetically favored state.

The apparent chemical shift of the hydroxyl protons of water molecules varies with the ratio of water to EO in the micelle, as shown by the open circles in Figure 7. When Z is increased, the apparent chemical shift δ first shows little change, then increases quickly, and finally tends toward a constant. This result is similar to that for poly(ethylene glycol) dodecyl ether in benzene.[18] In general, the solubilized water can be divided into free water and bound water. The free water molecules interact only between themselves; the bound water forms hydrogen bonds with oxyethylene. In the low Z region, most of the water forms hydrogen bonds with EO because formation of a water–EO hydrogen bond has priority in comparison with the energy of the water–water hydrogen bond.[17] The hydrogen bond energy of water–EO is about 22 kJ mol^{-1}, which is about 2.5 kJ mol^{-1} larger than the association energy per bond in a water trimer molecule.[7] After the Z value is increased to a certain value (Z_s), the EO has almost

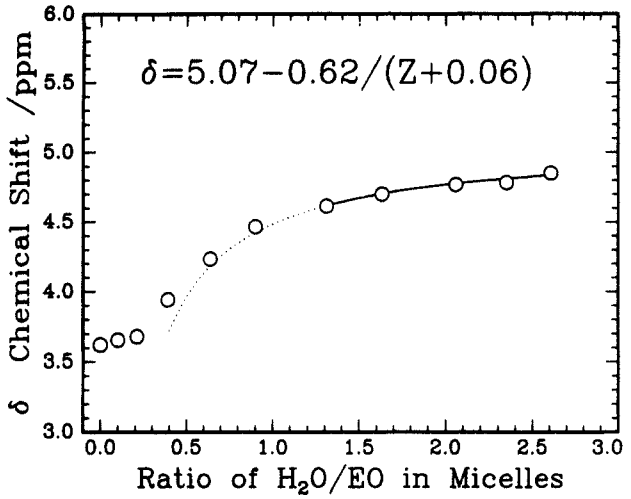

Figure 7. Apparent chemical shift of water protons as a function of water ratio (○). The solid line is a best fit of eq 16B. The dotted curve denotes an extension of eq 16B to $Z \approx 0.4$.

been saturated with water; the additional incoming water is free water capable of forming only hydrogen bonds with water. The experimentally measured apparent chemical shift represents an average contribution from all kinds of protons. If we know the chemical shift of free water (δ_f) and bound water (δ_b) as well as the molar fraction of bound water (Φ_b), we can calculate the apparent chemical shift δ by eq 13. After all EO units have been saturated, the chemical shift can be expressed as

$$\delta = \frac{0.15\text{cmc}\delta_b + (C - \text{cmc})(\delta_s Z_s + \delta_f(Z - Z_s))}{0.15\text{cmc} + (C - \text{cmc})Z} \quad (16)$$

where δ_s is an apparent chemical shift when all EO units have been saturated ($Z = Z_s$) and both δ_s and Z_s are constant. We assume that all the water molecules which interact with unimers are bound water and the ratio (0.15) remains unchanged. On substitution of $C = 0.316$ g cm^{-3}, and cmc $= 8.6 \times 10^{-2}$ g cm^{-3}, eq 16 becomes

$$\delta = \delta_f - \frac{(\delta_f - \delta_s)Z_s + 0.056(\delta_f - \delta_b)}{Z + 0.06} \quad (16B)$$

The solid line in Figure 7 is a result of fitting eq 16B. The fit agrees well with experimental data when $Z > 1.3$, implying that almost all EO have been saturated when $Z > 1.3$. The results are confirmed by the viscosity and light scattering results, as will be discussed later. From the fitting result, we calculate the chemical shift of free water, δ_f, to be 5.07 ± 0.04 ppm. In comparison with the known chemical shift of pure water, 5.14 ppm,[22] our result is reasonable for bulk water. Free water could really exist in the L64/*o*-xylene/water micelle.

From the NMR results, we can get some information about the mechanism of water solubilization in L64/*o*-xylene. When a small amount of water is present, almost all the water molecules are preferably bound with EO, and L64 exists in the unimer form. The NMR results suggest that when the water to EO ratio becomes larger (e.g., $Z > 0.2$), there is a competition for hydrogen bonding sites and thereby an equilibrium distribution between the bound and free water molecules. Free water molecules in an apolar medium tend to form clusters. The water clusters should function as nucleation centers to promote the association of L64 copolymer into micelles with end PEO blocks oriented toward the water clusters and the middle block extending into the apolar medium. Such a plausible mechanism is supported, as will be discussed later, by the static and dynamic light scattering results

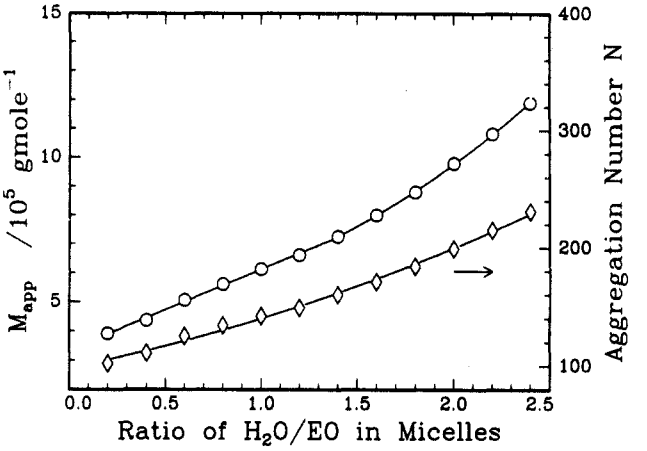

Figure 8. Weight average molar mass of the micelles and the corresponding aggregation number of the micelles as a function of water to EO ratio (Z) at 26.2 °C.

that instead of the L64 unimer with $R_h = 1.4$ nm in the region $Z < 0.2$, polymolecular micelles with an aggregation number of about 110 and $R_h \approx 9.2$ nm are formed when Z reaches about 0.4. Accordingly, the NMR spectra clearly display an enhanced, downfield shifted peak for the water protons due to the appearance of free water molecules, as shown in Figure 6.

(3) Light Scattering. Both static and dynamic light scattering were employed to study the association behavior of L64 in *o*-xylene in the presence of water. As in the case of anhydrous *o*-xylene, the scattered intensity of *o*-xylene solution of L64 with added water also showed no angular dependence. Hence, the R_{90} (excess value as compared to the R_{90} at cmc) results were used in the data analysis. We assume that the shape and size of micelles are independent of the micelle concentration when the molar ratio of water to EO units (Z) is fixed and that the cmc does not depend on Z. The systems studied were in the semidilute region. The HC/R_{90} versus C plot is no longer linear because the higher-order concentration terms are not negligible. But a semilogarithmic plot of HC/R_{90} versus C is linear (see eq 4C) within the concentration range used; therefore, we used the $\log(HC/R_{90})$ versus C plot (C is the concentration of micelles, i.e. L64 plus solubilized water, in g cm^{-3}) to extrapolate to the cmc value in order to get the molar mass of the micelles. From the slope, we can also estimate the approximate equivalent hard sphere size. We assume that all the micelles have the same composition at a given Z, and the measured apparent molar mass can be taken approximately as the weight-average molar mass of the micelle. The changes in the weight-average molar mass of the micelle and corresponding aggregation numbers with Z are shown in Figure 8, where three different regions of Z exist. In the first region ($Z \leq 0.10$), L64 exists in the form of unimers. With an increase in Z, M_w* shows a jump because of the formation of micelles and then M_w* steadily increases with increasing Z. When $Z < 1.4$ (second region), the rate of increase in M_w with Z remains relatively constant and is lower than that in the third region ($Z > 1.4$) although no clean discontinuity can be observed. Such multiregion behavior is also confirmed by dynamic light scattering measurements. As we would expect, the correlation functions show no angular dependence for R_h. For example, Figure 9 shows a typical size distribution of L64 micelles in the presence of water ($C = 0.186$ g cm^{-3}, $Z = 2.0$), measured at 45, 60, and 90° with a standard deviation of line width distribution in Γ space being 0.12, 0.16, and 0.23, respectively, indicating relatively narrow polydispersity in micellar size. Both the cumulants and

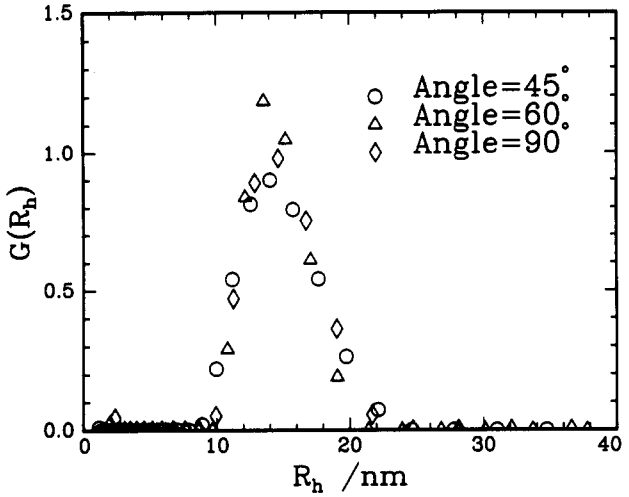

Figure 9. Size distribution curve of the micelles from CONTIN analysis at Z = 2.0. The concentration of L64 is 0.186 g cm^{-3}.

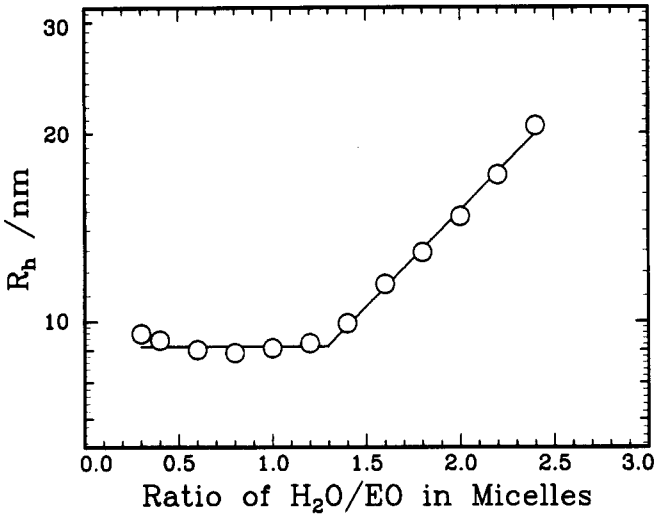

Figure 10. Plot of the hydrodynamic radius of the micelles at the cmc versus Z at 26.2 °C.

CONTIN methods were used to analyze the correlation function data. The results by these two methods agree well. Figure 10 shows R_h as a function of Z. There are also three regions: R_h is very small (Table I), R_h is nearly constant ($R_h \approx 9.2$ nm, $Z < 1.3$), and R_h increases with increasing Z.

The measured molar mass of the micelle consists of the weight of L64 and water. The aggregation number of the micelle, N, can be estimated by the relation

$$N = M_w/[M_0(1 + kZ)] \quad (17)$$

where k (=0.164) is the conversion coefficient and M_w and M_0 (=3.7 × 10^3 g mol^{-1}) are the weight-average molar mass of the micelle and of the unimer, respectively. If we assume that both PEO and water are located in the core of the micelle and the core is liquid-like, the core volume can be readily computed on the basis of the assumption of volume additivity. If the core has a spherical shape, the core radius is given by

$$R_C = \{3NM_0(V_{EO} + V_w)/(4\pi N_A)\}^{1/3} \quad (18)$$

where V_{EO} (=0.4/1.05 = 0.38 cm^3) and V_w (=(0.4/44)18Z = 0.164Z cm^3) are the volume of the EO unit and volume of solubilized water per gram of L64. The measured and calculated parameters of micelles are summarized in Table II. In Table II, the molar ratio of water to EO Z in the micelle, hydrodynamic radius (R_h), and the equivalent hard sphere radius (R_{HS}) are the measured results. N is the average aggregation number of micelles calculated with eq 17, R_η is an equivalent viscosity calculated with eq 12, and R_C is an equivalent core radius of micelles calculated with eq 18.

For $Z < 1.4$, the ratios of R_{HS}/R_h (ca. 0.8) and R_η/R_h (ca. 0.9) are almost constants. For $Z > 1.4$, both ratios decrease continuously with increasing Z. The change suggests that the micellar shape is different for $Z < 1.4$ and $Z > 1.4$. We suggest that micelles have a spherical shape when $Z < 1.4$ and become nonspherical, e.g. ellipsoids, when $Z > 1.4$. For a spherical particle, the ratio of R_{HS}/R_h or R_η/R_h should remain relatively constant when the conformation of the particle has remained relatively unchanged. For nonspherical particles, these size ratios are determined by particle shape. If the sphere model holds, the difference between the hydrodynamic radius and the equivalent core radius, $R_h - R_C$, a measure of the shell thickness of the micelle, should be nearly a constant. This is indeed the case when $Z < 1.4$, as shown in Table II. On the other hand, in the region $Z > 1.4$, the apparent shell thickness increases considerably with increasing Z, thus indicating that the sphere model is not valid in the region $Z > 1.4$. For unimer, Z simply denotes the water to EO ratio, while for micelle, Z denotes the water to EO ratio in the micelle.

From a consideration of the structure of the L64 molecule, we could also reach a similar conclusion. On the basis of the structure data, the bond length of C–C is 1.54 Å and that of C–O is 1.43 Å; the bond angle ∠OCC = ∠COC = 109.5°.[25] We can calculate the EO unit length of a zigzag conformation as 3.6 Å. The maximum stretched length of a PEO block is ca. 5.6–6.0 nm and of a PPO block is ca. 12.7–13.7 nm (MW ca. 3400–3700 g mol^{-1}). In an actual case, the maximum stretched length of PEO block could be shorter because the EO unit could also take another conformation (e.g. meander conformation), which has a shorter structure length (ca. 2.7 Å). It is not difficult to imagine that the micelle core consists of a concentrated PEO–water solution rather than one having a free-water pool at the center of the core and PEO shell.[28] As the core size, as well as the micelle size, are determined by the structure of the L64 block copolymer, the core radius will not be larger than the maximum stretched structure length of the PEO block (ca. 5.6–6.0 nm) and the micelle size cannot be larger than half of the maximum stretched structure length of L64 (ca. 12–12.8 nm) if the micelle has a spherical shape, but without a free-water pool in the PEO core. The volume of a micelle core increases with increasing Z (Table II, R_C). When Z is increased to a certain value, the micelle core volume becomes too large for a sphere with a radius equivalent to the maximum length with which the PEO block can reach. In order to avoid the formation of a free-water pool in the micelle core, it becomes necessary to change the micelle shape in order to increase the core volume. In the extreme cases ($Z > 1.8$), both the core volume and the micelle size are definitely larger than what a spherical micelle can provide. Thus a nonspherical shape for such micelles becomes a reasonable explanation. At low Z (e.g. $Z < 1.4$), the core volume is not too large to fit the spherical model. Therefore, the micelle is spherical in this region. Our results of $R_h \approx 9.2$ nm in this region are in agreement with the literature results of hydrodynamic radius of L64 micelles in water ($R_h \approx 8.5$,[5] 10,[2] and 9.2 nm[3]). More recent, transient electric birefringence (TEB) and small-angle X-ray scattering (SAXS) results[26] show that the micelle at high Z resembles an ellipsoid with a short axial ratio. The TEB and SAXS results agree with light scattering

Table II
Results of L64 in o-Xylene in the Presence of Water

Z	N	R_{HS} (nm)	R_h (nm)	R_{HS}/R_h	R_η (nm)	R_η/R_h	R_C (nm)	$R_h - R_C$ (nm)
0.2	102	7.2			7.5		4.0	
0.4	111	6.7	9.3	0.72	7.7	0.83	4.2	5.1
0.6	125	6.9	9.0	0.77	8.0	0.89	4.4	4.6
0.8	134	7.1	8.9	0.80	8.2	0.92	4.7	4.2
1.0	142	7.3	9.1	0.80	8.4	0.92	4.8	4.3
1.2	149	7.5	9.2	0.80	8.5	0.92	5.0	4.2
1.4	160	7.8	9.9	0.79	8.7	0.88	5.2	4.7
1.6	171	8.1	11.5	0.71	8.9	0.77	5.4	6.1
1.8	184	8.4	12.9	0.65	9.1	0.71	5.7	7.2
2.0	199	8.8	14.7	0.60	9.4	0.64	5.9	8.8
2.2	215	9.0	17.1	0.53	9.6	0.56	6.2	10.9
2.4	231	9.3	20.5	0.45	9.8	0.48	6.4	14.1

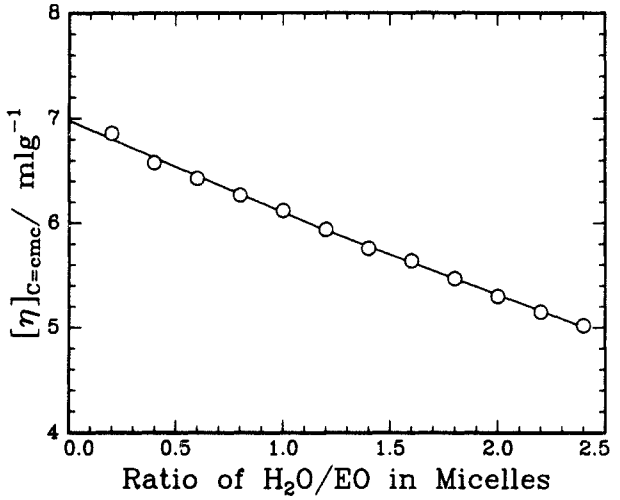

Figure 11. Intrinsic viscosity of L64 micelles in o-xylene at 26.2 °C as a function of water to EO ratio (Z) at the cmc.

results. The details will be presented in a separate article.

(4) Viscosity. We used a Brookfield cone-plate viscometer to measure the viscosity of L64 solutions at four concentrations (C = 0.289, 0.246, 0.192, and 0.152 g cm^{-3}, respectively) and at different Z values. We tried to measure the viscosity at different shear rates but did not observe a shear rate dependence within the range 1.15–230.0 s^{-1}. This is in agreement with the preliminary conclusions from the TEB and SAXS results[26] that, at high Z values, the ellipsoids formed exhibit a small axial asymmetry (e.g. axial ratio ≈ 3 when Z = 2.6). In the concentrations studied, the η_{sp}/C versus C plots show upturn curves, while those in a $\ln(\eta_r)/C$ versus C plot are linear. We used the $\ln(\eta_r)/C$ versus C plot to extrapolate to the zero micelle concentration in order to obtain $[\eta]$ at a given Z. Figure 11 shows the relationship between the intrinsic viscosity $[\eta]$ and Z. $[\eta]$ decreased with increasing Z. The rate of decrease in $[\eta]$ was barely lower in the high Z region. From eq 11, we know that both the degree of solvation and the particle shape could affect the intrinsic viscosity. A combination of NMR and light scattering results offers a possible explanation for the viscosity results as follows. For Z < 1.3, the micelle was spherical, as indicated by light scattering measurements, and therefore the degree of solvation of the micelle could be estimated by using eq 11. The weight fraction of the PPO block in the micelle, as defined by $W_{PPO}/(W_{L64} + W_{water}) = 0.6/(1 + 0.164Z)$, decreased with increasing Z. This decrease could suggest that the degree of solvation of the micelle was reduced with increasing Z while the solvated o-xylene molecules per PO unit remained nearly constant, as implied by the NMR results that the solubilized water resided with the PEO core in this region. For Z > 1.3, the degree of solvation was expected to decrease perhaps even faster with increasing Z. The micellar shape became increasingly asymmetric, yielding an opposite effect in the intrinsic viscosity. The combination of the two opposite effects (i.e., a decrease in the degree of solvation decreases the intrinsic viscosity while an increase in the asymmetry in the shape increases the intrinsic viscosity as shown in eq 11) could explain the decreasing rate in the high Z region. At the present time, it seems difficult to extract quantitative information, i.e. the axial ratio of the micelle, from the viscometry results.

Conclusions

From the study the L64/water/o-xylene system by light scattering, NMR, and viscometry, we can reach the following conclusions.

L64 does not form polymolecular micelles in the absence of water and in the presence of a small amount of water (H_2O/EO ≲ 0.15). However, L64 can form micelles when more water is present. The aggregation number and the structure of the micelles are determined by the amount of water added. There exist three regions for the water to EO ratio: Z < 0.2, 0.2 < Z < 1.3, and Z > 1.3. For Z < 0.2, L64 exists in the unimer form. When the ratio H_2O/EO is between 0.2 and 1.3, the hydrodynamic radius (ca. 9.2 nm) remains essentially unchanged, and the micelle has a spherical shape. When the ratio H_2O/EO is larger than 1.3, the aggregate number and the hydrodynamic radius increase with increasing Z, and correspondingly, the micelle may transform to an asymmetric shape. Again, it should be noted that the shape transition is not sharp, for example, in Figure 8, the discontinuity in slope can hardly be observed. Therefore, a value of Z ≈ 1.3 represents only a rough measure of the cross-over region. From the NMR results, we have found that water can be classified as bound water and free water. In the case that a large amount of water is present, water is not evenly distributed in the micelle core, and the environments of EO units along the PEO chains could be different.

Acknowledgment. We gratefully acknowledge support of this research by the Polymers Program, National Science Foundation (DMR 8921968), and the Department of Energy (DEFG0286ER45237.A008). G.W. wishes to thank Dr. Zhaoda Zhang for his help in NMR measurements.

References and Notes

(1) Schmolka, I. R. In *Nonionic Surfactants*; Shick, M. J., Ed.; Marcel Dekker: New York, 1967.
(2) Zhou, Z.; Chu, B. *J. Colloid Interface Sci.* **1988**, *126*, 171; *Macromolecules* **1987**, *20*, 3089; **1988**, *21*, 2548.
(3) Tontisakis, A.; Hilfiker, R.; Chu, B. *J. Colloid Interface Sci.* **1990**, *135*, 427.
(4) Reddy, N. K.; Fordham, P. J.; Attwood, D.; Booth, C. *J. Chem. Soc., Faraday Trans.* **1990**, *86*, 1569.

(5) (a) Brown, W.; Schillen, K.; Almgren, M.; Hvidt, S.; Bahadur, P. *J. Phys. Chem.* **1991**, *95*, 1850. (b) Almgren, M.; Stam, J. V.; Lindblad, C.; Li, P.; Stillbs, P.; Bahadur, P. *J. Phys. Chem.* **1991**, *95*, 5677. (c) Almgren, M.; Bahadur, P.; Jansson, M.; Li, P.; Brown, W.; Bahadur, A. *J. Colloid Interface Sci.* **1992**, *151*, 157.
(6) Wanka, G.; Hoffmann, H.; Ulbricht, W. *Colloid Polym. Sci.* **1990**, *268*, 101.
(7) (a) Alig, I.; Ebert, R. U.; Hergeth, W. D.; Wartewig, S. *Polym. Commun.* **1990**, *31*, 314. (b) Wartewig, S.; Alig, I.; Hergeth, W. D.; Lange, J.; Lochmann, R.; Scherzer, T. *J. Mol. Struct.* **1990**, *219*, 365.
(8) (a) Turro, N. J.; Chung, C. *Macromolecules* **1984**, *17*, 2123. (b) Turro, N. J.; Kuo, P. *J. Phys. Chem.* **1986**, *90*, 4205; *Langmuir* **1987**, *3*, 773.
(9) Attwood, D.; Rassing, J. *Int. J. Pharmaceutics* **1983**, *13*, 47.
(10) Almgren, M.; Alsins, J. *Langmuir* **1991**, *7*, 446.
(11) Prasad, K. N.; Luong, T. T.; Florence, A. T.; Paris, J.; Vaution, C.; Seiller, M.; Puisieux, F. *J. Colloid Interface Sci.* **1979**, *69*, 225.
(12) Al-saden, A. A.; Whateley, T. L.; Florence, A. T. *J. Colloid Interface Sci.* **1982**, *90*, 303.
(13) Cowie, J. M. G.; Sirianni, A. F. *J. Am. Oil Chem. Soc.* **1966**, *Oct.* 572.
(14) Samii, A. A.; Karlström, G.; Lindman, B. *Langmuir* **1991**, *7*, 1067; *Prog. Colloid Polym. Sci.* **1990**, *82*, 280.
(15) Friberg, S. E. In *Interfacial Phenomena in Apolar Media*; Eicke, H. F., Parfitt, G. D., Eds.; Marcel Dekker: New York, 1987.
(16) Ravey, J. C.; Buzier, M.; Picot, C. *J. Colloid Interface Sci.* **1984**, *97*, 9.
(17) Cooney, R. P.; Healy, T. W.; Barraclough, C. G. *J. Raman Spectrosc.* **1983**, *14*, 250.
(18) (a) Christenson, H.; Friberg, S. E.; Larsen, D. *J. Phys. Chem.* **1980**, *84*, 3633. (b) Christenson, H.; Friberg, S. E. *J. Colloid Interface Sci.* **1980**, *75*, 276.
(19) Chu, B.; Onclin, M.; Ford, J. R. *J. Phys. Chem.* **1984**, *88*, 6566.
(20) Benoit, H.; Froelich, D. In *Light Scattering from Polymer Solution*; Huglin, M. B., Ed.; Academic Press: New York, 1972.
(21) Tanford, C. *Physical Chemistry of Macromolecules*; John Wiley & Sons, Inc.: New York, 1961.
(22) Becker, E. D. *High Resolution NMR Theory and Chemical Application*, 2nd ed.; Academic Press: New York, 1980.
(23) Rodrigues, K.; Mattice, W. L. *Langmuir* **1992**, *8*, 456; *Polym. Bull.* **1991**, *25*, 239.
(24) (a) Cogan, K. A.; Gast, A. P. *Macromolecules* **1990**, *23*, 745. (b) Cogan, K. A.; Leermakers, F. A. M.; Gast, A. P. *Langmuir* **1992**, *8*, 429.
(25) Tadokoro, H. *Macromol. Rev.* **1967**, *1*, 119.
(26) Wu, G.; Zhou, Z.; Chu, B., in preparation.
(27) Percus, J. K.; Yevick, G. J. *Phys. Rev.* **1958**, *110*, 1.
(28) Nagarajan, R.; Ganesh, K. *Macromolecules* **1989**, *22*, 4312.